Chapter 2

TURBULENT DIFFUSION

Philip J. W. Roberts[1] and Donald R. Webster[2]

ABSTRACT

Almost all flows encountered by the engineer in the natural or built environment are turbulent, resulting in rapid mixing of contaminants introduced into them. Despite many years of intensive research into turbulent diffusion, however, our ability to predict mean contaminant distributions is often quite crude and to predict statistical variations of concentration fluctuations even cruder. This chapter reviews basic ideas of turbulence and the mechanisms whereby scalar quantities, such as contaminants, are mixed. The evolution equations for scalar quantities are derived, the engineering assumptions used to make them tractable are discussed, and typical solutions are presented. Applications to various situations of engineering interest are given, including diffusion in rivers, estuaries, and coastal waters. The complexities of the diffusion process are demonstrated by the use of new optical experimental techniques. New modeling techniques are discussed, and research questions are posed.

1. INTRODUCTION

Turbulent diffusion is very efficient in rapidly decreasing the concentrations of contaminants that are released into the natural environment. Despite intensive research over many years, however, only crude predictions of these concentrations can be made. Most mathematical models of turbulent diffusion, particularly engineering models, predict only time-averaged concentrations. While this may often be sufficient, for example, water quality standards are usually written in terms of time-averaged values, more information on the statistical variation of concentration fluctuations may sometimes be needed. This could include prediction of the peak exposures of humans to air pollutants, of aquatic organisms to water contaminants, of the probability of combustion of flammable gases accidentally released into the atmosphere, or of the information available to an organism attempting to navigate through a

[1] Professor, School of Civil and Environmental Engineering, Georgia Institute of Technology, Atlanta, Georgia 30332-0355, proberts@ce.gatech.edu
[2]Assistant Professor, *ibid*, dwebster@ce.gatech.edu

turbulent chemical odor plume to its source. These and similar topics are becoming increasingly important in turbulent diffusion research.

Consider the photograph of a passive tracer released into a turbulent flow shown in Figure 1. This photograph was obtained in a study of chemical odor plumes. Even a cursory inspection of this image shows that the time-average tracer concentration at any point would be a very poor measure of the contaminant signal there. This signal consists of a small mean value with intermittent fluctuations that range from zero to levels that are orders of magnitude higher than the mean. Present mathematical models usually do not predict higher order measures of these signals such as their intermittency, peak values, probability density functions, and spatial correlations.

Figure 1. Chemical plume released iso-kinetically into fully developed turbulent open-channel flow. The release height is ¼ of the channel depth.

New experimental techniques are now beginning to provide fresh insights into these questions. These include non-intrusive optical techniques, particularly planar laser-induced fluorescence (PLIF) to measure tracer concentration levels and particle image velocimetry (PIV) to measure velocity. They enable simultaneous measurement of instantaneous whole fields of tracer concentration and velocity from which detailed statistical measures of their spatial variability and correlations can be obtained. In this chapter, we will use some of these techniques to illustrate the complexities of turbulent diffusion.

The purpose of this chapter is to provide an introductory overview of the essential mechanisms of turbulent diffusion and some methods of predicting mean concentration distributions for a few select applications of engineering interest. We consider only the case of turbulent diffusion, that is, the spreading of a scalar quantity due to irregular turbulent velocity fluctuations. This excludes mixing due to the combined effect of diffusion plus shear in the mean velocity, sometimes known as shear-flow dispersion. We also exclude the effects of buoyancy due to density differences between the discharged fluid and the receiving fluid, and the suppression of turbulence due to density stratification. We first provide a review of turbulent flows, particularly those features that are important to turbulent diffusion. We then discuss the mechanisms whereby turbulence induces rapid mixing; derive the time-averaged equations of species conservation, and present methods of estimating the resulting turbulent diffusion coefficients. We then give examples of applications of interest to engineers and biologists. We conclude with a discussion of some of the newer techniques for turbulent diffusion simulations, and pose some research questions.

2. BASIC CHARACTERISTICS OF TURBULENT FLOWS

The first step in understanding turbulent diffusion and the fate of tracer concentrations is understanding some basic characteristics of turbulence.

2.1 The Nature of Turbulence

Turbulence is difficult to define exactly; nevertheless, there are several important characteristics that all turbulent flows possess. These characteristics include unpredictability, rapid diffusivity, high levels of fluctuating vorticity, and dissipation of kinetic energy.

The velocity at a point in a turbulent flow will appear to an observer to be "random" or "chaotic." The velocity is unpredictable in the sense that knowing the instantaneous velocity at some instant of time is insufficient to predict the velocity a short time later. A typical velocity record is shown in Figure 2.

The unpredictable nature of turbulence requires that we describe the motion through statistical measures. The velocity typically will be described as a time-averaged value plus some fluctuation. Time-average quantities are denoted with an over bar:

$$\overline{u} = \frac{1}{T}\int_0^T u\,dt \tag{1}$$

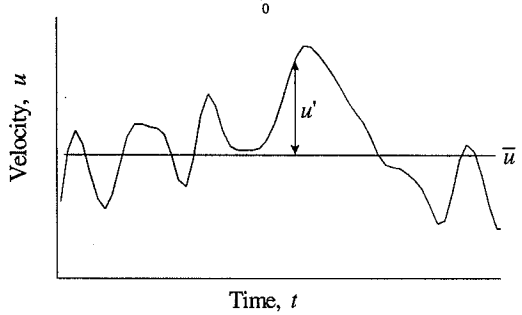

Figure 2. Sample turbulent velocity record.

where T is a time much longer than the longest turbulent fluctuations in the flow. A time record such as shown in Figure 2 is called statistically stationary if the mean quantities remain constant over the period of interest.

For a stationary velocity record, the instantaneous velocity can be decomposed into the sum of time-averaged and fluctuating contributions (called the Reynolds decomposition):

$$u = \overline{u} + u' \tag{2}$$

where u' is the fluctuating component (i.e. the deviation from the mean value) as shown in Figure 2. By definition, the time-average fluctuation is zero. Higher

order statistical quantities, such as the variance, are used to describe the magnitude of the fluctuations:

$$\tilde{u}^2 = \overline{u'^2} = \int_0^T (u - \bar{u})^2 \, dt \qquad (3)$$

The square root of the variance of the velocity fluctuations (the standard deviation, $\sqrt{\overline{u'^2}}$) is denoted by $\tilde{u}$ and is defined as the turbulence intensity.

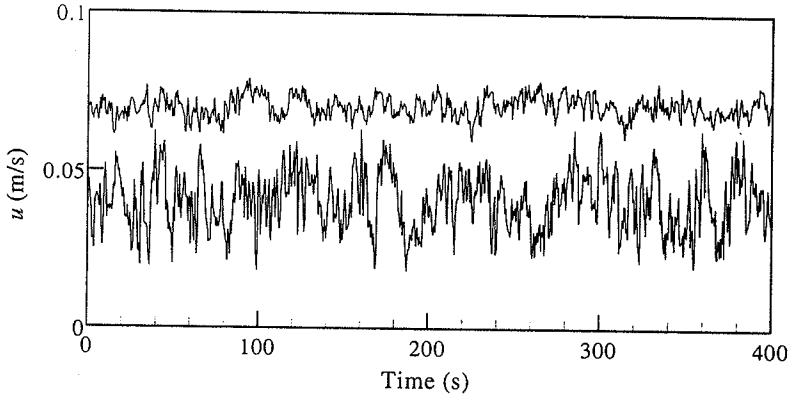

Figure 3. Velocity time series obtained in a turbulent open- channel flow at z/d=0.03 (bottom) and z/d=0.72 (top).

Actual velocity records obtained at two depths in the open channel flow photographed in Figure 1 are shown in Figure 3. The distance from the wall is z and water depth is d. The time-averaged velocity is greater farther from the wall, as would be expected in a boundary layer. The turbulence intensity also varies with distance from the wall, being significantly larger near the wall. The variation of the time-averaged velocity and turbulence intensity with distance from the lower bed are shown in Figure 4. The average velocity increases monotonically from zero at the wall; the turbulence intensity increases rapidly from zero at the wall to a local maximum near the wall and then monotonically decreases.

The velocity fluctuations act to efficiently transport momentum, heat, and tracer concentration. This turbulent transport is significantly more effective than molecular diffusion. Thus, the second characteristic of turbulence is a high rate of *diffusivity*. In fact, it is common to model the transport due to the fluctuations by defining an effective diffusion coefficient called the eddy diffusivity.

While the velocity fluctuations are unpredictable, they do possess a spatial structure. A turbulent flow, on close examination, consists of *high levels of fluctuating vorticity*. At any instant vortical motion, called eddies, are present in

the flow. These eddies range in size from the largest geometric scales of the flow down to small scales where molecular diffusion dominates. The eddies are

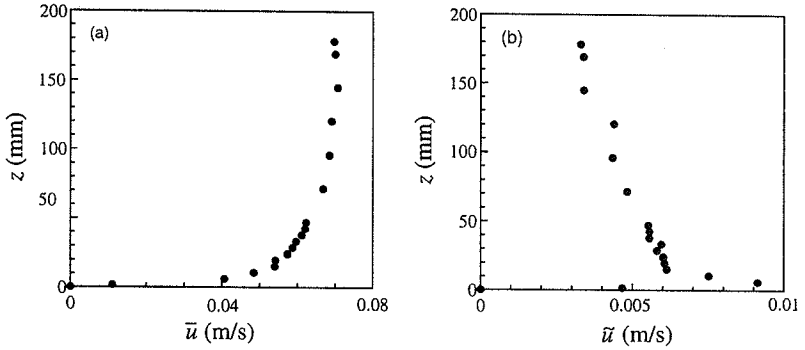

Figure 4. (a) Time-averaged, and (b) standard deviation velocity profiles for turbulent flow in an open-channel

continuously evolving in time, and the superposition of their induced motions leads to the fluctuating time records such as those shown in Figures 2 and 3. Turbulent kinetic energy is passed down from the largest eddies to the smallest though a process called the energy cascade. At the smallest scales, the energy is dissipated to heat by viscous effects. Thus, the fourth characteristic of turbulent flows is *dissipation of kinetic energy*. To maintain turbulence, a constant supply of energy must be fed to the turbulent fluctuations at the largest scales from the mean motion.

2.2 Length Sales in Turbulent Flows

Motions in a turbulent flow exist over a broad range of length and time scales. The length scales correspond to the fluctuating eddy motions that exist in turbulent flows. The largest scales are bounded by the geometric dimensions of the flow, for instance the diameter of a pipe or the depth of an open channel. These large scales are referred to as the *integral* length and time scales.

Observations indicate that eddies lose most of their energy after one or two overturns. Therefore, the rate of energy transferred from the largest eddies is proportional to their energy times their rotational frequency. The kinetic energy is proportional to the velocity squared, in this case the fluctuating velocity that is characterized by the standard deviation. The rotational frequency is proportional to the standard deviation of the velocity divided by the integral length scale. Thus, the rate of dissipation, ε, is of the order:

$$\varepsilon \propto \frac{\tilde{u}^3}{l} \qquad (4)$$

where l is the integral length scale.

Interestingly, the rate of dissipation is independent of the viscosity of the fluid and only depends on the large-scale motions. In contrast, the scale at which the dissipation occurs is strongly dependent on the fluid viscosity. These arguments allow an estimate of this dissipation scale, known as the Kolmogorov microscale, η, by combining the dissipation rate and kinematic viscosity in an expression with dimensions of length:

$$\eta \propto \left(\frac{\nu^3}{\varepsilon}\right)^{1/4} \tag{5}$$

Similarly, time and velocity scales of the smallest eddies can be formed:

$$\tau \propto \left(\frac{\nu}{\varepsilon}\right)^{1/2} \quad v \propto (\nu\varepsilon)^{1/4} \tag{6}$$

An analogous length scale can be estimated for the range at which molecular diffusion acts on a scalar quantity. This length scale is referred to as the Batchelor scale and it is proportional to the square root of the ratio of the molecular diffusivity, D, to the strain rate of the smallest velocity scales, γ:

$$L_B \propto \left(\frac{D}{\gamma}\right)^{1/2} \tag{7}$$

The strain rate of the smallest scales is proportional to the ratio of Kolmogorov velocity and length scales, $\gamma \propto v/\eta \propto (\varepsilon/\nu)^{1/2}$. Thus, the Batchelor length scale can be recast into a form that includes both the molecular diffusivity of the scalar and the kinematic viscosity:

$$L_B \propto \left(\frac{\nu D^2}{\varepsilon}\right)^{1/4} \tag{8}$$

The ratio of the Kolmogorov and Batchelor length scales equals the square root of the Schmidt number, Sc:

$$\frac{\eta}{L_B} \approx \left(\frac{\nu}{D}\right)^{1/2} \approx Sc^{1/2} \tag{9}$$

For the open channel flow example discussed in this chapter, the mean velocity is 50 mm/s and the integral length scale is roughly half the channel depth, i.e. 100 mm. The fluid was water at 20°C with a kinematic viscosity of $1\times10^{-6} m^2/s$. Therefore, the Kolmogorov length and time scales are 0.7 mm and 0.5 s, respectively. Assuming a diffusivity, $D = 1\times10^{-9} m^2/s$ for the chemical tracer photographed in Figure 1, the Batchelor scale is 0.02 mm, which is 35 times smaller than the Kolmogorov microscale. Thus, we would expect a much finer structure of the concentration field than the velocity field.

2.3 Energy Cascade

The energy spectrum characterizes the turbulent kinetic energy distribution as a function of length scale. (The power spectrum is usually

described in terms of a wave number, k, which is the inverse of length, but we will focus our discussion in terms of physical length scales.) The spectrum indicates the amount of turbulent kinetic energy contained at a specific length scale. This section describes some universal features of the energy spectrum for turbulent flows.

As described in the previous section, the large turbulent length scales in the flow dictate the rate of dissipation. These large length scales draw energy from the mean flow, then transfer the energy to successively smaller scales until it is dissipated at the Kolmogorov microscale. This process is called the *energy cascade*.

The energy distribution at the largest length scales is generally dictated by the flow geometry and mean flow speed. In contrast, the smallest length scales are many orders of magnitude smaller than the largest scales and hence are isotropic in nature. In between, we can describe an inertial subrange bounded above by the integral scale and below by the Kolmogorov microscale, $\eta \le L \le l$. In this range, the spectrum will only be a function of the length scale and the dissipation rate. (The spectrum depends on the dissipation rate because the largest length scales set the rate and the energy is transferred through this range.) With this dependence, dimensional reasoning yields Kolmogorov's $k^{-5/3}$ law:

$$E = \alpha\varepsilon^{2/3}k^{-5/3} \tag{10}$$

where k is the wavenumber and α is a constant of order one.

A typical energy spectrum is shown in Figure 5. The large length scales have the most energy and the distribution in that range depends on the boundary conditions. The smaller scales have less energy by several orders of magnitude. In between, the turbulent kinetic energy varies in the inertial subrange in proportion to $k^{-5/3}$. Also indicated in the figure is the Batchelor scale, which is more than an order of magnitude smaller than the Kolmogorov scale.

2.4 Evolution Equations

Turbulent flows must instantaneously satisfy conservation of mass and momentum. Thus, in principle, the incompressible continuity and Navier-Stokes equations can be solved for the instantaneous turbulent flow field. The difficulty with this approach is that an enormous range of scales must be accounted for in the calculation. To accurately simulate the turbulent field, the calculation must span from the largest geometric scales down to the Kolmogorov and Batchelor length scales. Even with the fastest, largest modern supercomputers, such a calculation can be achieved only for simple geometries at low Reynolds numbers. In many situations, engineers and scientists are satisfied with an accurate assessment of the time-averaged flow quantities. For instance, the time-averaged

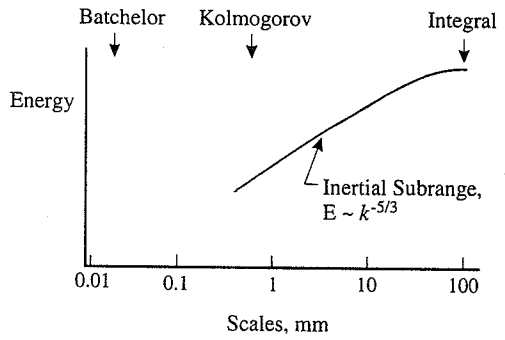

Figure 5. Typical turbulence energy spectrum, with length scales for the open channel flow of Figures 1 through 4 indicated.

velocity and pressure distribution is sufficient to calculate the wind load on a skyscraper. To derive the time-averaged flow equations we start with the instantaneous conservation equations, substitute the Reynolds decomposition (Eq. (2)), and time average the equations, yielding:

$$\frac{\partial \overline{u}_i}{\partial x_i} = 0 \tag{11}$$

$$\rho\left(\frac{\partial \overline{u}_i}{\partial t} + \overline{u}_j \frac{\partial \overline{u}_i}{\partial x_j}\right) = -\frac{\partial \overline{p}}{\partial x_i} + \mu \frac{\partial^2 \overline{u}_i}{\partial x_j^2} - \rho \frac{\partial}{\partial x_j}\overline{u_i' u_j'} \tag{12}$$

where we have employed indicial notation to indicate vectors and the standard Einstein summation convention. These Reynolds-averaged equations for the mean velocity and pressure are very similar to the instantaneous continuity and Navier-Stokes equations. The primary difference is the addition of the $\rho \frac{\partial}{\partial x_j}\left(\overline{u_i' u_j'}\right)$ term in the time-averaged momentum equation. This term is called the Reynolds stress tensor; it physically corresponds to the transport of momentum due to the turbulent fluctuations. This turbulent transport generally dominates that due to molecular diffusion. An equation for the time-averaged scalar transport equation can be derived in the same way, as will be shown in Section 3.3.

While the evolution equations for the time-averaged quantities are valid, they cannot be solved because several new unknown quantities have been introduced, specifically $\overline{u_i' u_j'}$. This dilemma is referred to as the "closure problem"; in other words, the mathematical problem is not closed because there are more unknowns than equations.

2.5 Turbulent Kinetic Energy Budget

An evolution equation for the kinetic energy can be derived for both the mean and turbulent components of the flow. The mean kinetic energy equation is:

$$\underbrace{\frac{D}{Dt}\left(\frac{1}{2}\overline{u}_i^2\right)}_{\substack{\text{total change in}\\ \text{mean kinetic energy}}} = \underbrace{\frac{\partial}{\partial x_j}\left(\frac{-\overline{p}\overline{u}_j}{\rho} + 2\nu \overline{u}_i S_{ij} - \overline{u_i' u_j'}\overline{u}_i\right)}_{\text{transport}} - \underbrace{2\nu S_{ij} S_{ij}}_{\substack{\text{viscous}\\ \text{dissipation}\\ \text{(typically small)}}} + \underbrace{\overline{u_i' u_j'}\frac{\partial \overline{u}_i}{\partial x_j}}_{\substack{\text{loss to}\\ \text{turbulence}}} \tag{13}$$

where $S_{ij} = \frac{1}{2}\left(\frac{\partial \overline{u}_i}{\partial x_j} + \frac{\partial \overline{u}_j}{\partial x_i}\right)$ is the mean strain rate tensor.

The equation indicates that the total change in kinetic energy of the mean flow results from the combined effects of transport, viscous dissipation, and loss to turbulence. The loss to turbulence is the dominant term on the right hand side of the equation. As discussed in the previous section, the mean flow feeds energy to the large turbulent scales. The viscous dissipation is generally small for the mean flow because the gradients of mean velocity are mild. The transport terms represent the spatial movement of mean kinetic energy.

The budget of turbulent kinetic energy is:

$$\underbrace{\frac{D}{Dt}\left(\frac{1}{2}\overline{u_i'^2}\right)}_{\substack{\text{total change in}\\ \text{turbulent kinetic energy}}} = \underbrace{\frac{\partial}{\partial x_j}\left(\frac{-\overline{p' u_j'}}{\rho} + 2\nu \overline{u_i s_{ij}} - \frac{1}{2}\overline{u_i'^2 u_j'}\right)}_{\text{transport}} - \underbrace{2\nu \overline{s_{ij} s_{ij}}}_{\substack{\text{viscous}\\ \text{dissipation}}} - \underbrace{\overline{u_i' u_j'}\frac{\partial \overline{u}_i}{\partial x_j}}_{\substack{\text{shear}\\ \text{production}}} \tag{14}$$

where $s_{ij} = \frac{1}{2}\left(\frac{\partial u_i'}{\partial x_j} + \frac{\partial u_j'}{\partial x_i}\right)$ is the strain rate tensor for the fluctuating field.

The shear production term is identical to the loss to turbulence term in the mean equation, although opposite in sign. These terms correspond to kinetic energy transfer from the mean scales to the turbulent scales. In this equation, the viscous dissipation is not small; in fact, the dissipation of turbulent kinetic energy is an important characteristic of every turbulent flow as discussed in the previous sections. Again, the transport terms correspond to the spatial movement of the turbulent kinetic energy.

3. MECHANISMS OF MIXING IN TURBULENT FLOWS

As the previous brief review has shown, turbulent flows contain irregular motions over a wide range of length and time scales. The major question in this chapter is: How do these motions contribute to mixing, resulting in the plume patterns seen in Figure 1 and the concomitant rapid decay of contaminant concentrations with distance from the source? In this section, we discuss these issues, and derive the equations of mass conservation in turbulent flows.

3.1 Molecular Diffusion

Consider first mass transport due to molecular diffusion. The rate of mass transport in the x-direction is given by Fick's law:

$$q = -D\frac{\partial c}{\partial x} \tag{15}$$

where q is the solute flux, i.e. the mass transport rate per unit area per unit time, c is the mass concentration, i.e. the mass of tracer per unit volume, and D is the molecular diffusion coefficient. Eq. (15) can be readily generalized to three dimensions:

$$\vec{q} = -D\vec{\nabla}c \tag{16}$$

where the arrows indicate vector quantities.

Eqs. (15) and (16) state that the rate of mass transport due to molecular diffusion in any direction is directly proportional to the concentration gradient in that direction. The equations are analogous to Fourier's law of heat conduction, which states that the heat (energy) flux due to conduction is proportional to the temperature gradient. In both cases, the negative sign indicates that the direction of transport is down the gradient (i.e. from hot to cold, or high to low concentration). For other transport processes, it is sometimes assumed that the flux is also proportional to the concentration gradient. These processes are then called Fickian processes, in analogy to Eq. (16), although the transport mechanism can be other than molecular diffusion.

In a flowing fluid, another major transport mechanism occurs due to the flow itself. The magnitude of this transport in the x-direction is uc, or more generally in three dimensions $\vec{u}c$. This is called advective transport. (It is often called convective transport, but we prefer to reserve the word convective for motions induced by buoyancy effects).

We can derive the equations for conservation of species by applying mass conservation to an arbitrarily-shaped control volume (see, for example, Fischer et al., 1979). The result, where the transport mechanisms are molecular diffusion and advective transport, is:

$$\frac{\partial c}{\partial t} + u\frac{\partial c}{\partial x} + v\frac{\partial c}{\partial y} + w\frac{\partial c}{\partial z} = D\left(\frac{\partial^2 c}{\partial x^2} + \frac{\partial^2 c}{\partial y^2} + \frac{\partial^2 c}{\partial z^2}\right) \tag{17}$$

This equation is known as the advective-diffusion equation and is closely analogous to the heat conduction equation. Because of this, solutions to similar heat conduction problems can sometimes be utilized in mass diffusion problems. Many solutions to the heat conduction equation are presented in the classic texts by Crank (1956), and Carslaw and Jaeger (1959). In addition, Fischer et al. (1979) discuss some fundamental properties of, and solutions to, the advective-diffusion equation.

The molecular diffusion coefficient, D, is a property of both the fluid and the diffusing solute. For low tracer concentrations (i.e. dilute solutions), D is constant, and values can be obtained from tables such as those in CRC Handbook of Chemistry and Physics (1999). For example, the diffusion coefficient for salt

(NaCl) diffusing into water is about 1.5×10^{-9} m^2/s. For gases diffusing into air the diffusion coefficient is much higher; for methane into air, it is about 1.8×10^{-5} m^2/s.

To illustrate the consequences of these values, consider the distance, L, diffused by some material in a time t given a diffusion coefficient D. Simple scaling indicates:

$$L \propto \sqrt{Dt} \quad \text{or} \quad t \sim \frac{L^2}{D} \tag{18}$$

Suppose this refers to sugar deposited at the bottom of a coffee cup. For a cup height of 5 cm, the time for sugar to become uniformly mixed through the cup by molecular diffusion is, from Eq. (18), of the order of 30 days! Clearly, molecular diffusion is a very slow process. The mechanism to produce full mixing quickly is known to all: Stir the coffee to produce advection and turbulence, which results in uniform mixing in a few seconds. If molecular diffusion were the only process acting to diffuse the plume shown in Figure 1 (i.e. if the channel flow were laminar), it would maintain it's identity as a thin streak with negligible mixing for very long distances from the source.

An important property of mixing is the relationship that exists between the variance of the spatial concentration distribution in a diffusing cloud in various situations to the diffusion coefficient. In Section 4, solutions to the advective-diffusion equation are presented for constant diffusion coefficients. In each case the concentration distribution is a Gaussian function proportional to $\exp\left(-r^2/4Dt\right)$, where r is the distance from the centerline. The standard deviation of the concentration distribution, σ (which is also a measure of the characteristic width of a plume) is therefore:

$$\sigma = \sqrt{2Dt}$$

which is consistent with the scaling of Eq. (18). It follows that

$$\frac{1}{2}\frac{d\sigma^2}{dt} = D \tag{19}$$

This result will be used later in the chapter when modeling the eddy diffusivity due to turbulent mixing.

3.2 Mixing In Turbulent Flows

So how does turbulence result in such rapid mixing? Consider a patch of material in a turbulent flow, as shown in Figure 6. Within the turbulent flow is a wide range of length scales, or eddy sizes, (Figure 5) ranging from the integral scale down to the Kolmogorov scale. Eddies that are smaller than the patch size down to the Kolmogorov scale. Eddies that are smaller than the patch size continually distort it resulting in steep concentration gradients, which are then smoothed by molecular diffusion. The role of eddies that are larger than the patch size is to translate the entire patch without contributing to its mixing. The mixing process is therefore due to distortion, stretching, and convolution of the original

patch whereby the original volume is distributed irregularly over a larger volume, so that the concentration, averaged over some finite volume, decreases. In the absence of molecular diffusion, however, such a process would not reduce actual peak concentrations at a point; the reduction of these peaks is therefore very dependent on molecular diffusion.

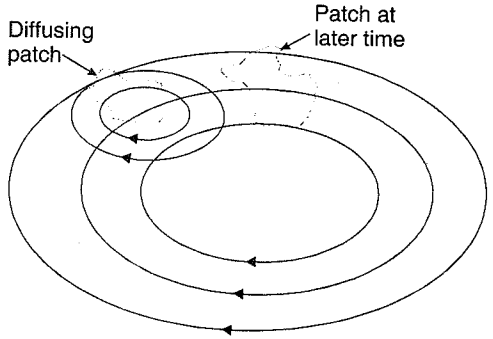

Figure 6. Schematic depiction of a patch diffusing in a turbulent flow.

3.3 Conservation Equations

We can derive a conservation equation for turbulent flows from the advective-diffusion equation by decomposing the velocity and concentration into the sum of their mean and fluctuating parts and then time-averaging the result. This is similar to the process whereby the evolution equations were derived in Section 2.4. Thus:

$$c = \overline{c} + c' \tag{20}$$

where $\overline{c}$ is the time-averaged concentration and c' the instantaneous fluctuation, or deviation, from the mean. On substituting this into Eq. (17), along with the velocity decompositions, (Eq. (2)), and time-averaging the result, we obtain:

$$\frac{\partial \overline{c}}{\partial t} + \overline{u}_j \frac{\partial \overline{c}}{\partial x_j} = D\frac{\partial^2 \overline{c}}{\partial x_j^2} - \frac{\partial}{\partial x_j}\overline{u_j' c'} \tag{21}$$

As before, the time-averaged transport equation is similar to the instantaneous equation (Eq. (17)) with the addition of the $\frac{\partial}{\partial x_j}\overline{u_j' c'}$ term, which physically corresponds to the transport of c by turbulent fluctuations. The x-component of the terms on the right-hand side of Eq. (21) can be written:

$$\frac{\partial}{\partial x}\left(D\frac{\partial \overline{c}}{\partial x} - \overline{u'c'} \right)$$

from which it can be seen that both terms in the parentheses represent mass transport. The first is the transport due to molecular diffusion (Fick's law, Eq. (15)), and the second is a turbulent flux that arises due to the correlation between

u' and c'. Because D is usually a very small quantity, $\overline{u'c'} >> -D\frac{\partial c}{\partial x}$ and the molecular transport term is neglected compared to the turbulent flux. Note, however, that molecular diffusion is still an important mechanism for mixing at the smallest scales, as discussed in Section 3.2.

It is usual to drop the bar terms at this point, so $c = \overline{c}$, and $u = \overline{u}$, etc., and Eq. (21) then becomes:

$$\frac{\partial c}{\partial t} + u\frac{\partial c}{\partial x} + v\frac{\partial c}{\partial y} + w\frac{\partial c}{\partial z} = -\frac{\partial}{\partial x}\overline{u'c'} - \frac{\partial}{\partial y}\overline{v'c'} - \frac{\partial}{\partial z}\overline{w'c'} \tag{22}$$

Again, this equation cannot be solved because three new unknown quantities have been introduced, specifically $\overline{u_i' c'}$. This is the "closure problem" again; in other words, the mathematical problem is not closed because there are more unknowns than equations. To circumvent this problem, the unknown quantities are often modeled, at least for common engineering problems, with eddy diffusivity coefficients, ε_i, defined as :

$$\overline{u'c'} = -\varepsilon_x \frac{\partial c}{\partial x} \qquad \overline{v'c'} = -\varepsilon_y \frac{\partial c}{\partial y} \qquad \overline{w'c'} = -\varepsilon_z \frac{\partial c}{\partial z} \tag{23}$$

Eq. (23) assumes that the diffusion process is Fickian, i.e. the turbulent mass transport is proportional to the mean concentration gradient. While this simple model can be effective, the coefficients are strongly flow dependent, vary within the flow field, and are not known a priori. As a result, estimation of eddy diffusivity coefficients often relies on empirical data.

As already stated, the turbulent transport is much greater than the molecular transport, i.e. $\varepsilon_i >> D$. With this assumption, Eq. (22) becomes:

$$\frac{\partial c}{\partial t} + u\frac{\partial c}{\partial x} + v\frac{\partial c}{\partial y} + w\frac{\partial c}{\partial z} = \frac{\partial}{\partial x}\left(\varepsilon_x \frac{\partial c}{\partial x} \right) + \frac{\partial}{\partial y}\left(\varepsilon_y \frac{\partial c}{\partial y} \right) + \frac{\partial}{\partial z}\left(\varepsilon_z \frac{\partial c}{\partial z} \right) \tag{24}$$

This equation is the most usual starting point for water and air quality models (with the possible addition of terms to account for creation and loss of species due to chemical or biological processes). The assumptions made in deriving it should be kept in mind, however.

When using Eq. (24), obvious questions are: what are the values of the eddy diffusion coefficients in any particular situation, and how do they depend on any reasonably obtained or measured mean properties of the flow? It should be reiterated that these coefficients are properties of the flow, and cannot therefore be found in any standard tables or handbooks of fluid properties.

3.4 Estimation of Eddy Diffusion Coefficients.

G. I. Taylor published one of the most important results in turbulent diffusion theory, which provides a link between the eddy diffusion coefficients and turbulent flow properties, in 1921. To illustrate his theory, consider two realizations of an experiment in which two particles are released into a turbulent flow, as sketched in Figure 7.

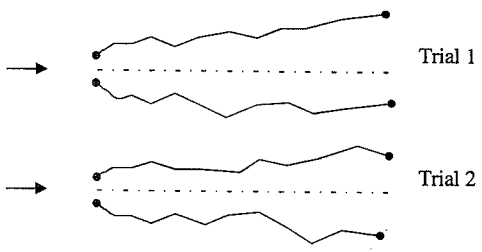

Figure 7. Trajectories of two particles released into a turbulent flow.

Because the turbulent velocity fluctuations are irregular, the results of each trial differ. On average, however, the particles wander apart from each other, and the rate at which they wander apart can be related to a diffusion coefficient. This is easier to imagine by considering individual particles, released from the coordinate origin at different times, as shown in Figure 8. The particle location after travel time T is:

$$\vec{X} = \int_0^T \vec{u} dt$$

where $\vec{u}$ is the velocity of the particle as it travels (i.e. its Lagrangian velocity).

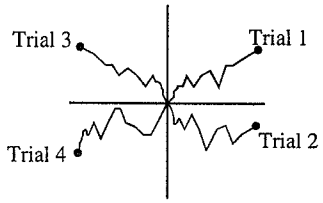

Figure 8. Possible trajectories of a particle released at the coordinate origin at various times into a turbulent flow.

The mean position of the particles, averaged over many releases in a stationary, homogeneous turbulent field, is clearly zero, i.e. the origin. The variance of their displacements is not zero, however, and is given by:

$$\overline{X^2(t)} = 2\tilde{u}^2 \int_o^t \int_o^{t'} R_L \, d\tau \, dt' \qquad (25)$$

where R_L is the autocorrelation of the velocity:

$$R_L(\tau) = \frac{\overline{u(t)u(t+\tau)}}{\tilde{u}^2} \qquad (26)$$

and $\tilde{u}^2 = \overline{u'(t)u'(t)}$ is the variance of the velocity fluctuations. The autocorrelation is a measure of the memory of the flow, in other words how well correlated future velocities are with the current value.

It would be expected that the shape of the autocorrelation function would have the form sketched in Figure 9. It should tend to zero for long times, in other words, the particle eventually "forgets" its original velocity. For short times, however, the velocity is strongly correlated with its original velocity.
We can define a time scale T_L for this process by:

$$T_L = \int_0^\infty R_L d\tau \qquad (27)$$

from which it can be seen that the area under the rectangle of width T_L is the same as that under the curve of. R_L. T_L is known as the Lagrangian time scale of the flow, and it gives rise to a definition of a Lagrangian length scale:

$$L_L = \tilde{u} T_L \qquad (28)$$

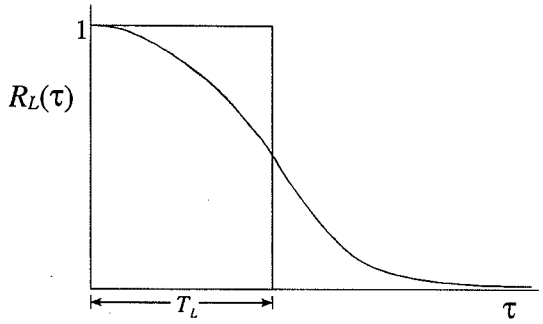

Figure 9. Autocorrelation function.

For times less than T_L and distances smaller than L_L, the velocities are generally well correlated and R_L approaches one. The Lagrangian length scale is closely related to the integral length scale, l, because the length over which the flow is well correlated corresponds to the size of the largest eddies.
We are interested in two limiting cases: very long times and very short times compared to T_L. For long times, (i.e. $t \propto T_L$) Eq. (25) becomes:

$$\overline{X^2(t)} = 2\tilde{u}^2 T_L t + \text{constant}$$

On differentiating this expression with respect to time, we obtain:

$$\frac{1}{2}\frac{d\overline{X^2(t)}}{dt} = \tilde{u}^2 T_L \tag{29}$$

The standard deviation of the displacement, $\sqrt{\overline{X^2(t)}}$, therefore increases in proportion to $t^{1/2}$ because the distance traveled is analogous to a random walk, that is, uncorrelated steps. By analogy to Eq. (19), the left hand side of Eq. (29) can be taken as a diffusion coefficient, therefore:

$$\varepsilon \propto \tilde{u}^2 T_L \propto \tilde{u} L_L \tag{30}$$

Taylor did not give a diffusion coefficient in his original analysis; also, Eq. (30) is only valid for travel times longer than T_L. An important consequence for this case is that the eddy diffusion coefficient is constant, as given by Eq. (30).

In the other limit of short travel times (i.e. $t \ll T_L$), the autocorrelation is very close to one ($R_L \approx 1$). Eq. (25) then becomes:

$$\overline{X^2(t)} = \tilde{u}^2 t^2$$

so the standard deviation of the displacements increases in proportion to t because of complete correlation between steps. On differentiation, this becomes:

$$\varepsilon = \frac{1}{2}\frac{d\overline{X^2(t)}}{dt} = \frac{1}{2}\tilde{u}^2 t \tag{31}$$

The diffusion coefficient is therefore not constant for short travel times; it increases in proportion to time because the particle displacements are highly correlated and the standard deviation of the displacement increases linearly.

For practical problems, it is more convenient to discuss the variation of the diffusion coefficient with patch or cloud size. Over a time T_L, a particle travels an rms distance $\tilde{u}T_L$. But $\tilde{u}T_L$ is the Lagrangian length scale L_L (Eq. (28)), so in other words the size of the diffusing cloud, L, should be much larger than the Lagrangian length scale, L_L for Eq. (30) to apply and for the diffusion coefficient to be constant. For smaller clouds, i.e. $L < L_L$, the diffusion coefficient increases with cloud size, and for very small clouds, Eq. (31) applies.

This result implies that the diffusion coefficient increases with cloud size while the cloud size is smaller than L_L. This phenomenon is known as relative diffusion – in other words, the magnitude of the diffusion coefficient is relative to the cloud size. When the patch size lies within the inertial subrange, Batchelor (1952) shows that the rate of increase of the mean square separation of the particles is:

$$\frac{d\overline{s^2}}{dt} \propto \varepsilon^{1/3}\left[\overline{s^2}\right]^{2/3} \tag{32}$$

where s is the separation between particles. This leads to the celebrated "4/3 power law" for diffusion:

$$\varepsilon = \alpha L^{4/3} \tag{33}$$

where α is a constant depending on the energy dissipation rate, and L is a measure of the cloud size. A similar result was first obtained by Richardson (1926) in conjunction with atmospheric diffusion. Equation 33 is frequently used for open water and atmospheric diffusion problems.

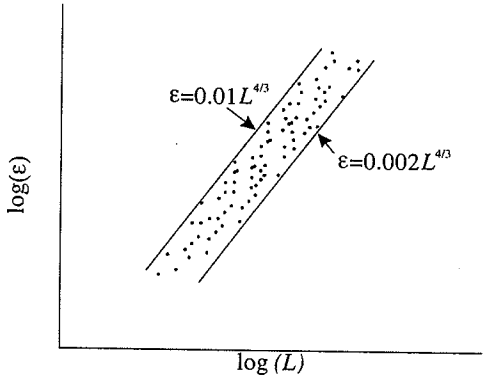

Figure 10. Relative diffusion in the ocean.

Observations of diffusing dye patches in the open ocean show considerable scatter when compared to Eq. (33). Some results are shown in Figure 10. The experiments can be approximately bracketed with $0.01 < \alpha < 0.002$ cm$^{2/3}$/s (see Fischer et al., 1979, Figure 3.5), ε in cm^2/s, and L in cm.

4. SOLUTIONS TO THE ADVECTIVE-DIFFUSION EQUATION

4.1 Introduction

In this section, we present solutions to the advective-diffusion equation (Eq. (17)) for several simple boundary and initial conditions. These solutions, while idealized, provide insight into the basic transport mechanism and provide a means for understanding situations that are more complex. Solutions provided here are referenced in future sections regarding specific flow applications.

4.2 Continuous Line Source In Two-Dimensions, Constant Diffusion Coefficient

Consider a steady release of contaminated fluid from a line source into a steady uniform flow with $\vec{u} = (U,0,0)$ as shown in Figure 11. The objective is to predict the concentration distribution in the x-y plane. This configuration models, for example, a continuous release into a deep river from a long multiport diffuser. The mass flow rate from the source per unit length along the z-axis is $\dot{m}$ (e.g. the units of $\dot{m}$ are kg/m/s). As the transport due to diffusion is significantly greater in the y-direction than in the x-direction, due to the steeper concentration gradients in the y-direction, the governing equation reduces to:

$$u\frac{\partial c}{\partial x} = D\frac{\partial^2 c}{\partial y^2}$$

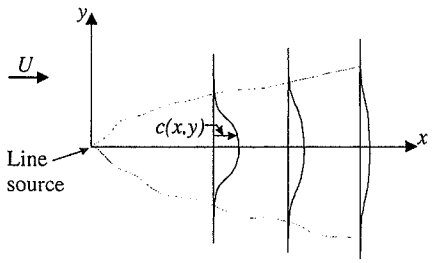

Figure 11. Diffusion from a continuous line source.

Applying the transformation $x = Ut$ yields the simple one-dimensional diffusion equation:

$$\frac{\partial c}{\partial t} = D\frac{\partial^2 c}{\partial y^2}$$

Let us first consider solutions to this equation by means of dimensional analysis. The downstream mean concentration is given by:

$$c = f\left(y, t, \dot{m}/U, D\right)$$

where $\dot{m}/U$ is the amount of mass of the contaminant "picked up" by the passing flow at the source. The concentration at any point in the field must be proportional to the contaminant mass flowrate divided by some characteristic length. Equation 18 defines a characteristic length, proportional to the distance that the contaminant diffuses in time t, $\sqrt{Dt}$. Thus,

$$c(y,t) = \frac{\dot{m}}{U\sqrt{4\pi Dt}} f\left(\frac{y}{\sqrt{4Dt}}\right)$$

where we have added arbitrary constants to make the solution mathematically more convenient. Inserting this functional form into the governing equation and defining a similarity variable, $\eta = y/\sqrt{4Dt}$, yields an ordinary differential equation whose solution is:

$$c(y,t) = \frac{\dot{m}}{U\sqrt{4\pi Dt}} \exp\left(-\frac{y^2}{4Dt}\right)$$

Finally, transforming back into spatial coordinates, $t = x/U$, we obtain:

$$c(x,y) = \frac{\dot{m}}{U\sqrt{4\pi Dx/U}} \exp\left(-\frac{y^2 U}{4Dx}\right) \qquad (34)$$

The solution at several distances from the line source is sketched on Figure 11. As the contaminant advects downstream in the x-direction, diffusion acts to spread the contaminant in the y-direction and decrease the centerline value in proportion to $x^{-1/2}$.

4.3 Continuous Point Source, Constant Diffusion Coefficient

Consider now a variation of the previous example in which a point source is exchanged for the line source (Figure 12). Among other examples, this configuration corresponds approximately to release from a smokestack into a crossflow. Define $\dot{m}$ as the mass flow rate from the source (whose units are now kg/s). Again, the velocity field is uniform flow in the x-direction, $\vec{u} = (U,0,0)$. The solution is analogous to the previous example except the contaminant spreads in the z-direction as well as the y-direction. The solution is:

$$c(x,y,z) = \frac{\dot{m}}{4\pi Dx} \exp\left(-\frac{\left(y^2+z^2\right)U}{4Dx}\right) \qquad (35)$$

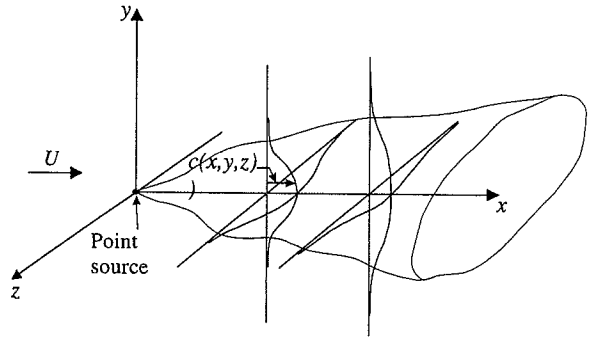

Figure 12. Diffusion from a continuous point source.

The concentration distributions at several distances downstream are sketched on Figure 12. The centerline concentration decreases more rapidly than for the line source as the distribution spreads in both the z- and y-directions; it decreases in proportion to x^{-1}.

In each of these examples it was assumed that the streamwise diffusion was negligible compared to the cross-stream diffusion. Close to the source, this assumption is not valid. Thus, the solutions discussed above are only valid for $x >> 2D/U$.

4.4 Continuous Line Source of Finite Length - Variable Diffusion Coefficient

This situation arises when sewage or other wastewaters are discharged from outfalls with fairly long diffusers into essentially unbounded waters such as a wide estuary or coastal waters (Roberts, 1996) as sketched in Figure 13. For this case, the advective-diffusion equation, Eq. (24), can be formulated as:

$$u\frac{\partial c}{\partial x}=\frac{\partial}{\partial y}\left(\varepsilon_y\frac{\partial c}{\partial y}\right)-kc \tag{36}$$

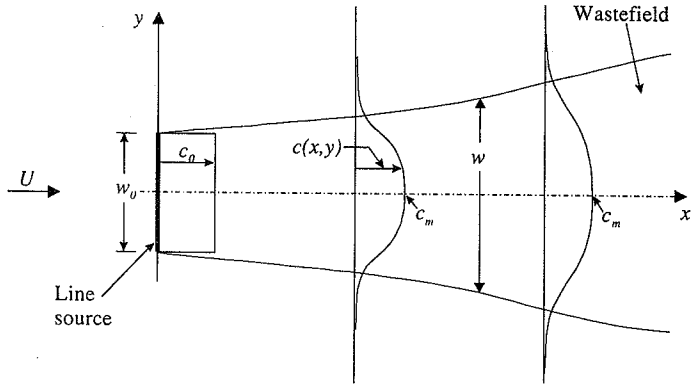

Figure 13. Diffusion from a continuous line source of finite length.

where we have assumed steady-state conditions and neglected diffusion in the x- and z-directions. Also, because bacterial decay is important for sewage discharges, we have included a decay term, $-kc$, which corresponds to a first-order decay process with k the decay constant. For zero decay, i.e. a conservative substance, the following solutions still apply with k set equal to zero.

Solutions to Eq. (36) for various assumptions about the variation of the diffusion coefficient ε_y were obtained by Brooks (1960). He defined the wastewater field width, w, in terms of the second moment of the concentration distribution, σ:

$$w=12\sigma^2=12\frac{\int_{-\infty}^{\infty}y^2c(x,y)dy}{\int_{-\infty}^{\infty}c(x,y)dy} \tag{37}$$

so that w, and therefore ε_y, are functions of x only. Assuming that ε_y follows the "4/3 law", Eq. (33), Brooks obtained the solution to Eq. (36) as:

$$c(x,y)=\frac{c_0e^{-kt}}{2\sqrt{\pi\varepsilon_0t'}}\int_{-w_o/2}^{w_o/2}\exp\left[-\frac{(y-y')^2}{4\varepsilon_0t'}\right]dy' \tag{38}$$

where $t = x/U$ and $t' = x'/U$ and x' satisfies the equation:

$$\frac{dx'}{dx}=\frac{\varepsilon}{\varepsilon_0}=\left(\frac{w}{w_o}\right)^{4/3}$$

where w_o is the length of the diffuser. Of particular interest is the centerline (maximum), concentration, c_m. This is obtained by putting $y = 0$ into Eq. (38), yielding:

$$c_m(x)=c_0e^{-kt}erf\sqrt{\frac{3/2}{\left(1+\frac{2}{3}\beta\frac{x}{w_o}\right)^3-1}} \tag{39}$$

where β is $12\varepsilon_o/Uw_o$ and $erf(\eta)=\frac{2}{\sqrt{\pi}}\int_0^{\eta}e^{-y^2}dy$ is the standard error function. For large distances from the source, i.e. $\beta\frac{x}{w_o}>>1$, Eq. (39) can be approximated by:

$$c_m(x)\approx c_0\frac{9}{2\sqrt{\pi}}\left(\beta\frac{x}{w_o}\right)^{-3/2}e^{-kt} \tag{40}$$

The variation of the wastewater field width is given by:

$$\frac{w}{w_o}=\left(1+\frac{2}{3}\beta\frac{x}{w_o}\right)^{3/2} \tag{41}$$

The implications of this solution will be discussed further in Section 6.2.

5. EXAMPLE: POINT SOURCE DIFFUSION

To illustrate the complexities and effects of turbulent diffusion, we consider a relatively well-defined situation: the diffusion from a small source in a turbulent shear flow. This is the case shown in Figure 1, which is an iso-kinetically released plume in a smooth bed, open-channel flow. The idealized mean concentration field for a constant diffusion coefficient is given by Eq. (35).

The instantaneous concentration field is much more complex, however. Using planar laser-induced fluorescence (PLIF), detailed spatial measurements of the instantaneous tracer concentration within the plume were obtained. (For details of the methodology and further results, see Webster et al., 1999, and Rahman et al., 2000). A typical instantaneous concentration distribution is shown in Figure 14.

It is clear that the concentration distribution is extremely patchy, with isolated pockets of high concentration that have steep gradients at their edges. In between the patches are large expanses with zero concentration. By averaging over many images similar to that shown in Figure 14, the time-averaged concentration field can be obtained, as shown in Figure 15. This distribution varies smoothly in space with moderate spatial concentration gradients, in contrast to the patchy instantaneous distribution.

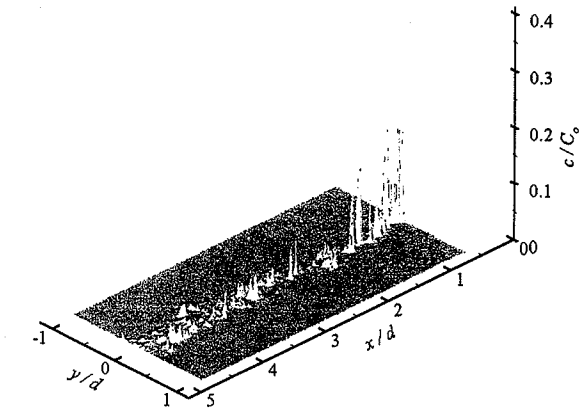

Figure 14. Instantaneous concentration distribution in a plane on the centerline of a plume in an open channel flow.

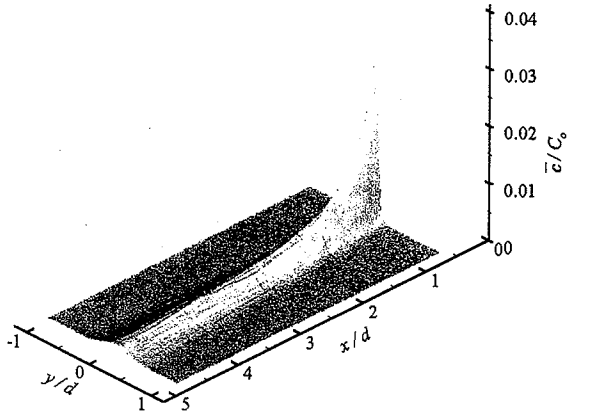

Figure 15. Time-averaged concentration distribution in a plane on the centerline of a plume in an open-channel flow.

A comparison of Figures 14 and 15 (note the different vertical scales) shows the peak concentration values on the centerline to be around an order of magnitude greater than the time-averaged values. Presumably, this ratio would be even higher off the plume axis, where time-averaged values decrease, but peaks can still be comparable to centerline values. It should be noted that peak values are very dependant on the sample size; peak values increase with decreasing sample size until the smallest concentration scale, the Batchelor scale, is reached.

For this case, the Batchelor scale is about 0.02 mm (Section 2.2) and the sample size about 1 mm, so the actual peaks could be much higher than those shown in Figure 14, and the peak to time-average ratios even higher.

The time-average and standard deviation of the concentration fluctuations along the plume centerline are shown in Figure 16. The time-averaged concentration decreases very rapidly with distance. This can be thought of in kinematic terms as the spreading of a fixed mass of tracer over an increasing volume by the action of the various eddy sizes. Initially, the time-average value decreases more rapidly than x^{-1} (see Eq. (35)), which indicates a relative diffusion regime. Between x/d = 2 and 5, the time-averaged concentration decreases approximately in proportion to x^{-1}, which agrees with Eq. (35) and

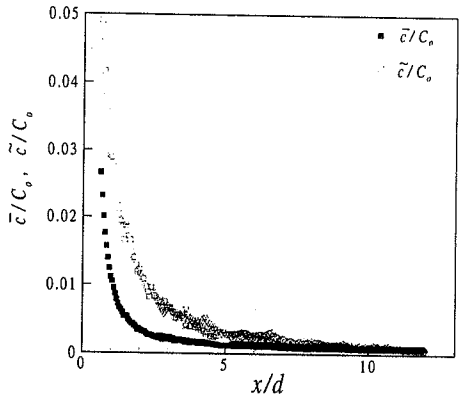

Figure 16. Variation of concentration properties along centerline of a plume in an open-channel flow.

implies a constant diffusion coefficient. Beyond x/d = 5, the rate of dilution slows, which suggests that the plume mixing may be influenced by the free surface and bed.

The standard deviation of the concentration fluctuations is greater than the time-average values along the centerline because, as seen in Figure 14, the concentration field consists of very large, but brief, spikes of concentration resulting in large fluctuations about the mean. The equations discussed previously (for example, Eq. (24)) only apply to time-averaged values and cannot predict the evolution of the concentration fluctuations. The behavior of these fluctuations is now receiving increasing attention, with additional measurements and further attempts to model them. A conservation equation for concentration fluctuations can be derived in a similar manner to that of turbulent kinetic energy (Eq. (14)). For the idealized case of a steady point source, the equation is (Pasquill and Smith, 1983):

$$\bar{u}\frac{\partial \overline{c'^2}}{\partial x} = -2\left[\overline{w'c'}\frac{\partial \bar{c}}{\partial z} + \overline{v'c'}\frac{\partial \bar{c}}{\partial y}\right] - \left[\frac{\partial}{\partial z}\overline{w'c'^2} + \frac{\partial}{\partial y}\overline{v'c'^2}\right] - S \qquad (42)$$

where S is the rate of reduction of the mean square fluctuations by molecular diffusion. Equation 42 makes the usual assumptions that gradients in the x-direction can be neglected compared to those in the y and z directions. Because of the usual closure problems, Eq. (42) cannot be solved directly. Some solutions, with certain assumptions, are given by Csanady (1967ab). Gifford (1959) proposed a model for atmospheric diffusion in which the plume is represented as discs in a plane normal to the mean wind speed.

Several studies have been reported in which concentration fluctuations were measured. The motivation for these studies includes pollution transport, boundary layer meteorology, and chemical plume tracking. Measurements of chemical plumes released into turbulent boundary layers in the laboratory (Fackrell and Robins, 1982; Nakamura, 1987; Bara et al., 1992; and Yee et al., 1993) and field (Gifford, 1960; Murlis and Jones, 1981; Jones, 1983; Murlis, 1986; Hanna and Insley, 1989; and Mylne et al., 1996) show highly intermittent concentration time-records. The intermittency is a result of the filamentous and unpredictable nature of the plume as illustrated in Figure 1. Measurements have typically consisted of time records of temperature or concentration at individual points in the flow, which have been analyzed to meet the specific focus of the study. For instance, Yee et al. (1993) attempted to match standard PDF shapes to their concentration record, while Murlis (1996) examined the importance of burst duration and intermittency to moth plume tracking. The new experimental techniques, for example PLIF, are now being applied to measure the spatial variation of instantaneous concentration distributions for the first time. These data should provide new insight into the instantaneous plume structure and enable more rigorous testing of models of the mixing and dilution processes.

6. APPLICATIONS

6.1 Rivers

A common civil and environmental application of turbulent diffusion theory is prediction of the mixing of pollutants in rivers and streams. Because of the importance of this topic, it has been extensively researched over many years.

Consider first the idealized case of mixing of a continuous discharge from a point source in a straight, rectangular channel of constant cross-section as shown in Figure 17. For steady-state conditions, longitudinal diffusion is small compared to longitudinal advection, i.e. $\frac{\partial}{\partial x}\left(\varepsilon_x \frac{\partial c}{\partial x}\right) << u\frac{\partial c}{\partial x}$. The mean transverse and vertical velocities, v and w, are zero so the advective-diffusion equation, Eq. (24), reduces to:

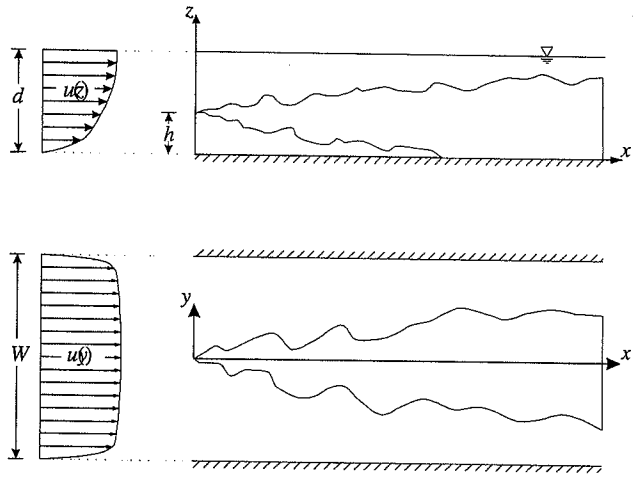

Figure 17. Diffusion from a point source into a straight, rectangular channel.

$$u\frac{\partial c}{\partial x} = \frac{\partial}{\partial y}\left(\varepsilon_y \frac{\partial c}{\partial y}\right) + \frac{\partial}{\partial z}\left(\varepsilon_z \frac{\partial c}{\partial z}\right) \qquad (43)$$

in which ε_y and ε_z are the transverse and vertical diffusion coefficients. The problem is now reduced to determination of ε_y and ε_z and their dependency on the turbulence characteristics of the flow.

Turbulence in open-channel flows has been extensively studied. The measurements of turbulence intensity shown in Figure 18 are typical. This is the same data shown in Figure 4b replotted in normalized form as $\tilde{u}/u^*$ where u^* is the friction velocity, defined as $u^* = \sqrt{\tau_o/\rho}$, where τ_o is the wall shear stress, and ρ the water density. It can be seen that $\tilde{u}$ is of the same order as u^*.

The largest length scales, or eddy sizes, of the turbulence in an open channel flow are smaller than the channel depth, d. A typical value is around half the channel depth. Thus, when the plume size becomes comparable to the depth, the diffusion coefficients are constant and Eq. (30) applies. Applying $\tilde{u} \propto u^*$ and $L_L \propto d$ to Eq. (30) we obtain:

$$\varepsilon_y \propto du^* \quad \text{and} \quad \varepsilon_z \propto du^* \qquad (44)$$

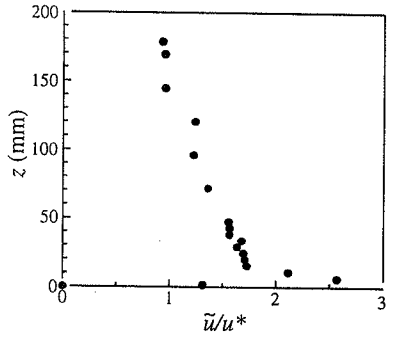

Figure 18. Normalized turbulence intensity for flow over a smooth bed open-channel flow.

Both the eddy length scales and the turbulence intensity vary over the depth, therefore, the vertical diffusion coefficient, ε_z, also varies with depth. The variation of ε_z with depth can be obtained by means of the "Reynolds analogy" whereby it is assumed that the mass diffusion coefficients are the same as the momentum diffusion coefficients. Using this assumption and a logarithmic velocity profile, Elder (1959) obtained the following expression for the depth-averaged value of ε_z for wide, open-channel flows:

$$\overline{\varepsilon_z} = 0.067 du* \tag{45}$$

and this result has been experimentally confirmed in a flume by Jobson and Sayre (1970).

If the channel is narrow relative to the depth, then the channel walls can affect the turbulence and transverse diffusion coefficient, ε_y. A more general statement of Eq. (44) for transverse mixing is then:

$$\frac{\varepsilon_y}{du*} = f\left(\frac{W}{d}\right) \tag{46}$$

where W is the channel width. Many experiments have been reported to evaluate the effect of W/d. The experiments performed up to 1979 are summarized in Fischer et al. (1979), which show the value of $\varepsilon_y/du*$ to range between 0.1 and 0.2 with no systematic dependence on W/d. Based on these results, Fischer et al. (1979) recommended use of the formula $\varepsilon_y = 0.15 du* \pm 50\%$; in other words, there is the possibility of an error of ±50% when using this formula.

More recent experiments have looked more carefully at the role of channel width and also the friction factor on lateral turbulent diffusion. Webel and Schatzman (1984) reported that if the flow is fully rough and $W/d \geq 5$ the walls exert no influence. For this case, Eq. (46) becomes (Webel and Schatzman, 1984):

$$\frac{\varepsilon_y}{du*} = 0.13 \tag{47}$$

As W/d decreases below about five, the wall effect causes the value of $\varepsilon_y/du*$ to increase. Discharges in the wall region, which extends for a distance of about $2.5d$ from the wall, experience a higher diffusion coefficient than releases in the center of the channel. They also find that diffusion dominates lateral mixing for straight laboratory channels. These findings were confirmed in Nokes and Wood (1988) in which it was suggested that $\varepsilon_y/du* = 0.134$ is a lower bound for lateral diffusion when the chief mixing mechanism is turbulence generated at the channel floor. This value applies for wide channels, and becomes independent of the friction factor, f, for $f > 0.055$. Nokes and Wood (1988) found the diffusion coefficient to be independent of the channel width when $W/d > 8$.

Natural streams differ from these ideal channels in at least three major ways. First is that the cross-section may vary irregularly, second the channel will probably meander and not be straight, and third there may be large sidewall irregularities. The effect of these on vertical mixing is not known, and we know of no experiments in which vertical mixing has been measured in the field. It is usual to assume that Eq. (45) also applies to natural channels. As will be shown later, vertical mixing in rivers is usually quite rapid compared with transverse mixing and precise quantification of the rate of vertical mixing is not usually important.

Bends and sidewall irregularities generally increase the rate of transverse mixing. A previous summary of much field data on mixing in rivers (see Fischer et al. (1979), table 5.2), shows that $\varepsilon_y/du*$ ranges between about 0.3 and 0.8 for reasonably straight channels. Most rivers fall in the range 0.4 to 0.8, and Fischer et al. (1979) recommends using:

$$\frac{\varepsilon_y}{du*} = 0.6 \pm 50\% \tag{48}$$

in the absence of any better information or field measurements. This equation is quite useful in that it contains only hydraulic parameters that can be fairly readily estimated for any particular river.

A bend in a river causes secondary circulations due to centrifugal forces, as shown in Figure 19. Such circulations would clearly considerably increase the rate of lateral mixing, which is now due to both advection and turbulent diffusion. If experimental results are parameterized as turbulent diffusion, the apparent diffusion coefficient increases markedly if the river is sharply curving. In a stretch of the Missouri River which included a 90° and a 180° bend, Yotsukura and Sayre (1976) found $\varepsilon_y/du* \approx 3.4$. Similarly high values of $\varepsilon_y/du*$ between 3.0 and 4.9 were also reported in a very sinuous section of the Ogeechee River by Pernik (1985), and in field tests on the Mississippi River (Dematracopoulos and Stefan, 1983) values between 0.24 and 4.65 were observed. The large transverse coefficients reported by Holly and Nerat (1983) suggest that secondary currents can play an important role in transverse mixing, and that the secondary

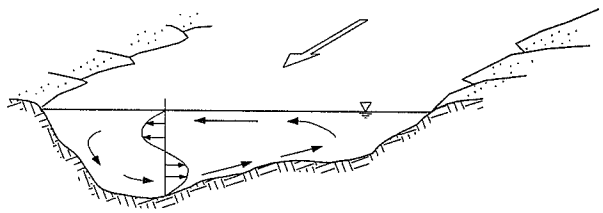

Figure 19. Secondary circulation in river bends.

circulations must be accounted for explicitly. A classification scheme, which can be used to indicate whether secondary currents will be strong enough to induce additional transverse transport, was presented by Almquist and Holley (1985).

It can be seen that our ability to predict diffusion coefficients is quite limited. If reliable knowledge of the value of ε_y is needed in a particular case, it will be necessary to perform a field experiment to measure it directly.

In order to apply Eqs. 45, 47, and 48, to rivers or any open channel flow, knowledge of u^* is necessary. Various empirical equations can be used to estimate u^*, including:

$$u^* = \left(gR_h S\right)^{1/2} \tag{49}$$

$$u^* = 3.1nUR_h^{-1/6} \quad \text{[SI units only]} \tag{50}$$

where g is the acceleration due to gravity, R_h is the hydraulic radius equal to the cross-sectional area divided by the wetted perimeter, S is the river slope, and n is the Manning coefficient. If the river slope is not known, Eq. (50) must be used. These equations pose yet another problem: what is the value of n?

Manning's coefficient, n, is a type of roughness parameter and its estimation for rivers is probably more of an art than a science. Some guidance is given, however, by books such as Chow (1950) in which values of n for various rivers are quoted. For natural streams the values range from about 0.025 for clean and straight sections up to 0.15 for very weedy and vegetated reaches. Streams wider than about 30 m have somewhat smaller n values. Flood plains can have very high n values, up to 0.2, especially if covered with heavy strands of trees. Other excellent sources of information on n values are Barnes (1967) and Arcement and Schneider (1984). Both these publications contain color photographs of rivers and their computed n values. It may be possible to find a river in these publications similar to the one of interest.

The implications of the results quoted above for mixing in typical rivers can be illustrated by means of an example. Let us consider first the rates with which materials mix vertically and transversely. The time, t, required for an effluent to mix a distance L with a diffusion coefficient ε is given by Eq. (18): $t \propto L^2/\varepsilon$. Thus, the ratio of the time required to mix transversely across the river, t_y, to that required to mix vertically, t_z, is:

$$\frac{t_y}{t_z} = \frac{\left(W/d\right)^2}{\left(\varepsilon_y/\varepsilon_z\right)^2} \tag{51}$$

To make this definite, suppose we have a channel with dimensions 30 m wide by 1 m deep. According to Eqs. 45 and 48, $\varepsilon_y/\varepsilon_z \approx 10$, so Eq. (51) becomes: $t_y/t_z \propto 90$. Thus, material mixes over the depth much quicker than it mixes across the width. This is a fairly typical result, and we usually go one step further to assume that vertical mixing is instantaneous compared to horizontal. Because of this relatively rapid vertical mixing, it will often be found that there is little variation in properties such as temperature over the depth of a river.

Consider, for example, the discharge from a point source in the middle of a river. Assuming the vertical mixing to be instantaneous is equivalent to replacing the source by a line source extending over the depth of the river. The problem is then two-dimensional, and when the plume size becomes comparable to the river depth the diffusion coefficient becomes constant, so Eq. (43) becomes:

$$U\frac{\partial c}{\partial x} = \varepsilon_y \frac{\partial^2 c}{\partial y^2} \tag{52}$$

Note that we have changed our notation slightly so that c is the time-averaged value and U is now the average river velocity equal to Q/A where Q is the river discharge and A the cross-sectional area. The solution to this equation for a steady release into a steady, uniform current is (Eq. (34)):

$$c = \frac{\dot{m}}{Ud\left(4\pi\varepsilon_y x/U\right)^{1/2}} \exp\left(-\frac{y^2}{4\varepsilon_y x/U}\right) \tag{53}$$

for an infinitely wide river, where $\dot{m}$ is the mass flow rate of pollutant. The maximum concentration occurs on the plume centerline (y = 0), and the concentration distribution about the maximum is a Gaussian, or normal, distribution. The plume width, w, is usually defined as four standard deviations of the Gaussian distribution, which is:

$$w = 4\left(2\varepsilon_y x/U\right)^{1/2} \tag{54}$$

So the plume grows in proportion to $x^{1/2}$ downstream and therefore reaches the banks, i.e. $w = W$, at a distance x_1 downstream given by:

$$x_1 = \frac{UW^2}{32\varepsilon_y} \tag{55}$$

Beyond this distance, Eq. (53) no longer applies as the effects of the banks must be considered. The rather lengthy analytical solution for this case is given in Fischer et al. (1979) (Eq. (5.9)). We rarely need the equation in this full form, however, as we are mostly concerned with the variation of maximum concentration, bank concentration, and the distance for uniform mixing. It is shown in Fischer et al. (1979) that these can be expressed in non-dimensional

form as in Figure 20. The non-dimensional distance is $x' = x\varepsilon_y / UW^2$ and concentration is expressed as c/c_o where c_o is the far-field concentration when the effluent is well-mixed over the river cross-section; it is given by $c_o = \dot{m}/UdW$.

Theoretically, the distance at which the plume becomes uniformly mixed over the river cross-section is infinite. Figure 20 shows, however, that for a dimensionless downstream distance x' greater than about 0.1, the concentration varies by less than 5% of the mean over the cross-section. Taking this to define the length, L_c, required for "complete mixing" we obtain:

$$L_c = 0.1\frac{UW^2}{\varepsilon_y} \tag{56}$$

for a centerline discharge. A comparison of Eqs. (55) and (56) shows that the distance for complete mixing is about three times the distance at which the plume first reaches the banks.

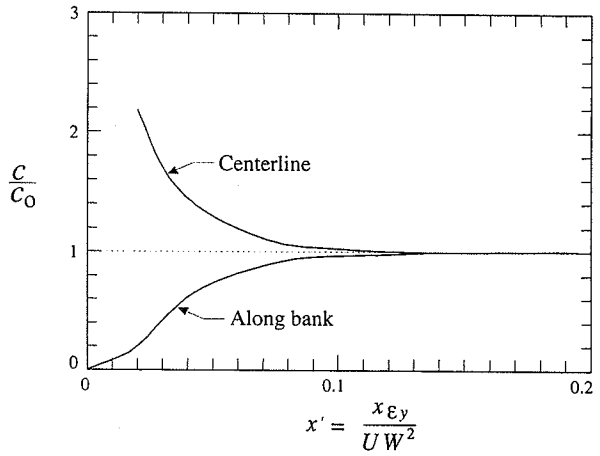

Figure 20. Downstream variation in tracer concentration resulting from a continuous point source into a river of uniform depth and velocity.

If the discharge is at one of the banks, the distance required for complete mixing increases. This distance can be obtained by replacing W in Eq. (56) by $2W$:

$$L_s = 0.4\frac{UW^2}{\varepsilon_y} \tag{57}$$

In other words, a side-discharge requires four times the distance for complete mixing than does a centerline discharge. (Assuming the lateral diffusion coefficient is constant across the channel. In actuality, it is somewhat higher near

the banks, so the ratio will be somewhat less than four times). Clearly, however, if it is necessary to discharge effluent from an open-ended pipe more rapid mixing will be accomplished by placing the discharge in the center of the river.

What are these distances for mixing in typical rivers? Suppose we have a discharge of effluent in the middle of a river flowing with an average speed U of 0.4 m/s that is 300 m wide and 3 m deep. The hydraulic radius, R_h, is 2.9 m. Assuming the Manning coefficient is 0.04, Eq. (50) gives the shear velocity, u^* = 0.042 m/s. Note that the shear velocity is roughly one tenth of the mean velocity, a fairly typical result. The diffusion coefficients are, from Eqs. 45 and 48, $\overline{\varepsilon_z} \approx 0.0084$ m^2/s, and $\varepsilon_y \approx 0.076$ m^2/s. For a bottom discharge, the distance required for the effluent to be mixed over the depth can be crudely estimated by replacing W with d and ε_y with ε_z in Eq. (57). The result implies that the effluent will be well-mixed vertically about 170 m downstream of the injection point.

The distance x_1 at which the plume reaches the river banks can be estimated from Eq. (55). Substituting the values above, we obtain $x_1 \approx 14{,}800$ m or about 15 km! The distance for uniform mixing from Eq. (56) is $L_c \approx 47{,}400$ m or 47 km. Clearly, these distances are very much greater than the distance for vertical mixing, justifying our assumption of two-dimensionality or very rapid vertical mixing.

These distances are probably surprisingly large to someone approaching the subject for the first time. The downstream distance where the plume reaches the banks is about fifty river widths, i.e. the plume remains slender for long distances downstream. A photograph of just such a case is given in Fischer et al. (1979), p. 115. Of course, in a real river, bends, cross-sectional changes, or other obstructions, could speed up the mixing. Nevertheless, this example shows that caution should be used in applying one-dimensional models right from the source, or in assuming very rapid cross-sectional mixing. It also shows the value of a multiport diffuser across the river that can cause this mixing to occur very rapidly.

The solution, Eq. (53), to the advective-diffusion equation, Eq. (24), is one of the simplest possibilities, and is given mainly for illustrative purposes. It is not possible in this review to give other solutions, but Holley and Jirka (1986), Ch. 5, provide solutions to other one-, two-, and three-dimensional problems.

Another method of analyzing diffusion in rivers is the ray method of Smith (1981). The depth topography can have a strong influence on lateral spreading, and use of the ray method shows that contaminant concentration is greatest in shallow water and towards the outside of bends.

6.2 Estuaries and Coastal Waters

Diffusion in estuaries and coastal waters has a number of applications, including prediction of mixing of wastewater discharges from sewage treatment plants, thermal effluent from power plants, and accidentally released oil spills.

For shallow waters, it is often assumed that the equation for open channels, Eq. (48) applies. This seems reasonable for cases where the turbulence is predominantly generated by bottom shear. For deeper waters other formulations are usually used. For a fairy small source in the initial stages of growth, Csanady (1973) recommends a constant diffusion coefficient $\varepsilon \approx 0.1$ m^2/s. For longer travel times or for larger source sizes, diffusion coefficients can be much larger, and the size of the source can significantly affect the rate at which it diffuses. Equation 39 is often used to model this situation. This solution assumes a line source of finite length and a variable diffusion coefficient that varies as the 4/3 power of plume size. Diffusion is two-dimensional, i.e. in the lateral direction only. Because the presence of density stratification inhibits vertical diffusion, this is a reasonable, and conservative, assumption. The dilution can be expressed as a far-field dilution $S_f = c_o / c_m$ where c_o is the initial concentration of some tracer (assumed uniform along the line source), and c_m is the maximum (centerline) concentration at some distance from the source. Rearranging Eq. (39) for a conservative constituent, i.e. $k = 0$:

$$S_f = \left[erf\left(\frac{3/2}{(1 + 8\alpha L^{-2/3} t)^3 - 1} \right)^{1/2} \right]^{-1} \qquad (58)$$

Equation (58) shows that the far field dilution depends only on the travel time, t. It is useful for examining the role of turbulent diffusion for diffusers of various lengths. Some computed values of the far-field dilution S_f assuming an upper value for α of 0.01 cm$^{2/3}$/s, are given in Table 1.

It can be seen that, whereas dilution by oceanic turbulence can be quite effective for short diffusers, it is relatively minor for long diffusers. The physical interpretation of this result is that the time needed for the centerline concentration to be reduced is the time required for eddies at the plume edges to "bite" into it. For a wide field produced by a long diffuser, the eddies have farther to go so it takes them longer to get to the centerline. The rate of decay is much smaller than for a small point source, for example, Figure 15.

	Far field dilution, S_f	
Travel time, t (hr)	Diffuser length, L (m)	
	35	700
1	2.4	1.0
3	7.4	1.4
10	35.5	3.2
20	95.9	6.9

Table 1. Far field dilutions for diffusers of various lengths.

6.3 Chemical Plume Tracking

Many aquatic and terrestrial animals rely on sensory cues to track turbulent odor plumes in order to locate food and mates. It is not practical for animals, such as blue crabs, to use the time-averaged concentration because they do not monitor the plume at a particular location long enough to obtain converged statistics (Elkinton et al., 1984, Moore and Atema, 1991). Thus, these animals must be using instantaneous observations of the odor plume to make tracking decisions. In this section, we discuss the usefulness of a sensory cue, namely bilateral comparison, available to animals such as blue crabs in a turbulent odor plume (Webster et al., 2001).

Animals, such as blue crabs and lobsters, have chemosensors on their appendages, which are separated horizontally. Several investigators have hypothesized that animals may be using bilateral comparison of these chemosensors to orient toward the source location (e.g. Reeder and Ache, 1980, Atema, 1996). To assess the usefulness of bilateral comparison, we evaluate the plume data presented in Section 5. Figure 21a shows the spatial correlation between the instantaneous centerline concentration, c_o, and the instantaneous concentration at distance y from the centerline, c_y. The correlation is identically one at the centerline and decreases rapidly with increased spacing because the dimensions of dye filaments are smaller than the sensor spacing. The area under the correlation curve increases dramatically as the plume grows downstream.

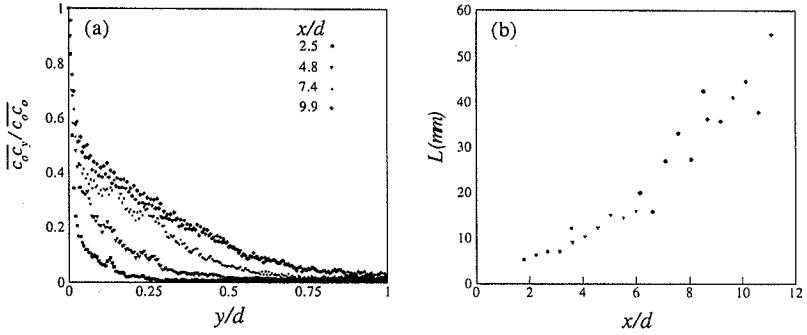

Figure 21. (a) Spanwise spatial correlation of absolute concentration at four locations. (b) Spanwise integral length scale.

This trend can be quantified by defining an integral spanwise length scale, L, calculated from the area under the correlation curve. As shown in figure 21b, this integral length scale increases with distance from the source. A searcher with sensors separated by a distance larger than the integral length scale, L, can better assess the instantaneous gradients and therefore identify the plume centerline more easily. In other words, with sensor spacing greater than the integral length scale, L, the searcher has sufficient spatial contrast to adjust toward the centerline of the plume from instantaneous measurements. With smaller sensor spacing, the

contrast is insufficient to make useful decisions based on the instantaneous concentration field. Since the plume is growing downstream, there is an advantage to animals that can continually maintain sensor spacing greater than L by either moving an appendage or having a broad array of sensors. This conclusion is consistent with Weissburg (2000), who defined the spatial integration factor (SIF) as the dimensionless ratio of the sensor spacing to the plume width and suggested that a large SIF allows the detection of a plume edge.

7. OTHER MODELING TECHNIQUES

7.1 Random Walk

The analytical solutions presented in Sections 4 and 6, while being very useful in providing insight into turbulent diffusion processes, are quite limited in practice. They only apply for flows with uniform and steady velocity, uniform diffusion coefficient, and simple geometries. They can also only predict mean concentration distributions. For real water quality problems, numerical, computer-based solutions are usually used. These fall into two main types.

First is numerical solution of the advective-diffusion equation, Eq. (24). Decay or production of species due to chemical, biological, or other processes can be readily incorporated (for example, the biological decay term in Eq. (36)), and multiple species and their chemical interactions can also be added. A separate hydrodynamic model is needed which is solved first to obtain the velocity field; this velocity field is then provided as input to the water quality model. An example of this procedure for coastal waters is given by Connolly et al. (1999).

The second major type is particle tracking, or random-walk models. In these models, mass is represented by discrete particles; at each timestep, the displacement of the particle follows a "random-walk." Following the description of Feynman et al. (1963) we can imagine a particle moving such that there is no correlation between the directions of two consecutive steps. In each timestep the particle moves a distance that is random with a Gaussian distribution and an average value L. After N steps, the rms distance traveled is proportional to the square root of the number of steps:

$$R_N^{rms} = L\sqrt{N}$$

As N is synonymous with time, this result is consistent with the observation in Section 3.1 that the distance diffused is proportional to $t^{1/2}$. This result is useful in relation to the eddy diffusivity model for times longer than the Lagrangian time scale, Eq. (30). In a flowing fluid, the displacement consists of an advective, deterministic, component and an independent random component. Again, the deterministic component must be supplied by a separate hydrodynamic model.

Random walk models have been extensively used in groundwater problems, and are now being increasingly used in surface water problems. We cannot review them in detail here, but they have been applied to rivers (Jeng and Holley, 1986, Pearce et al. 1990), to estuaries and coastal waters (Chin and Roberts, 1985, Dimou and Adams, 1994), and to the atmosphere (Luhar and Britter, 1992, Luhar and Sawford, 1995). Many more examples can be found in the literature.

8. FUTURE RESEARCH ISSUES

Probably the biggest research advance in recent years has been the rapid development of experimental instrumentation and computers. The rapid development of computers is familiar to all; their increasing power has led to their widespread use to solve diffusion problems of increasing complexity. The range of problems that can be solved continues to grow, but full solutions of the turbulent equations over the entire range of length scales in practical flows is still not in sight.

Perhaps less familiar is the rapid development of experimental techniques and instrumentation for both laboratory and field experiments. In the laboratory, the use of LIF is particularly useful, for example, the techniques that led up to Figures 14, 15, and 16. These optical techniques allow measurement with non-intrusive optical techniques of one million points or more simultaneously, at rates of 60 Hz or greater. Vast amounts of tracer concentration data can therefore be obtained. These can be combined with PIV techniques, which allow similar whole-field measurements of instantaneous velocity. The measurements of instantaneous concentration and velocity allow computation of mean values, but also many other properties, for example, their fluctuations, spatial correlations, and fluxes (Webster et al., 2001). These instrumentation advances result, in turn, from rapid advances in CCD sensors, image processing and acquisition, mass storage, and increasing computer power. These will undoubtedly continue in the future and should prove especially useful in conjunction with the development of mathematical turbulence models.

At the same time, field instrumentation has also rapidly developed. It is now possible to perform real-time monitoring of mixing in water environments with submersible fluorometers combined with packages that also measure currents, turbulence, and other properties (Petrenko et al., 1998, Roldao et al., 2000).

Demands on turbulence diffusion theory are now coming from new areas. For example, prediction of how animals or robots can seek the source of a turbulent chemical odor plume (Weissburg and Zimmer-Faust, 1994), and prediction of peak exposures of animals and organisms to contaminants. These require knowledge of characteristics that are not usually sought, for example, peak concentrations, probability density functions of concentration fluctuations, burst length and structure, and intermittency.

9. CONCLUSIONS

Turbulent diffusion is a complex process that is very efficient at mixing pollutants in the natural environment thereby reducing the concentrations of

potentially harmful contaminants to safe levels. Despite many years of research, it is still poorly understood, and can only be rather crudely predicted in many cases. In this chapter, we have given an introductory overview of the most important features of turbulence relevant to turbulent diffusion, and the processes whereby it occurs. We presented the equations for species conservation, and gave their solutions and examples in simple cases. Mathematical modeling techniques were briefly introduced for more complex situations.

Demands for more reliable predictions, and predictions of quantities that have received little attention in the past are now increasing. These are driven by increasing environmental awareness, more stringent environmental standards, and application of diffusion theory in new areas. These lead to the need to quantify and predict, for example, instantaneous peak concentrations, intermittency of concentration fluctuations, the durations of concentration bursts, their onset slopes, and many other characteristics.

One of the most exciting areas of diffusion research is the rapid development of instrumentation techniques in the laboratory and field. These have improved our ability to measure concentration fields enormously over the past ten years or so. The challenge now is to incorporate these new data into improved understanding and improved mathematical models of turbulent diffusion.

REFERENCES

Almquist, C. W., and Holley, E. R. (1985). "Transverse Mixing in Meandering Laboratory Channels with Rectangular and Naturally Varying Cross Sections." Report 205, Center for Research in Water Resources, Univ. of Texas at Austin, Austin, Texas.

Arcement, G. J., and Schneider, V. R. (1984). "Guide for Selecting Manning's Roughness Coefficients for Natural Channels and Flood Plains." Report No. FHWA-TS-84-204, U.S. Dept. of Transportation, Federal Highway Administration.

Atema, J. (1996). "Eddy Chemotaxis and Odor Landscapes: Exploration of Nature with Animal Sensors." *Biol. Bull.*, 191, 129-138.

Bara, B.M., Wilson, D.J., and Zelt, B.W. (1992). "Concentration Fluctuation Profiles from a Water Channel Simulation of a Ground-level Release." *Atmospheric Environment*, 26A, 1053-1062.

Barnes, H. H. (1967). "Roughness Characteristics of Natural Channels." Water Supply Paper 1849, U.S. Geological Survey.

Batchelor, G. K. (1952). "Diffusion in a Field of Homogeneous Turbulence. II. The Relative Motion of Particles." *Proc. Camb. Phil. Soc.*, 48, 345-362.

Brooks, N. H. (1960). "Diffusion of Sewage Effluent in an Ocean Current." *First International Conference on Waste Disposal in the Marine Environment*, pp. 246-267, University of California, 1959.

CRC Handbook of Chemistry and Physics (1999).

Carslaw, H. S. and Jaeger, J. C. (1959). *Heat Conduction in Solids*, Oxford University Press, Second Edition.

Chin, D. A., and Roberts, P. J. W. (1985). "Model of Dispersion in Coastal Waters." *J. Hydr. Eng.*, ASCE, 111(1), 12-28.

Chow, V. T. (1950). *Open-Channel Hydraulics*, McGraw-Hill.

Connolly, J. P., Blumberg, A. F., and Quadrini, J. D. (1999). "Modeling Fate of Pathogenic Organisms in Coastal Waters of Oahu, Hawaii." *Journal of Environmental Engineering*, ASCE, 125(5), 398-406.

Crank, J. (1956). *The Mathematics of Diffusion*, Oxford University Press.

Csanady, G. T. (1967a). "Concentration Fluctuations in Turbulent Diffusion." *J. Atm. Sc.*, 24, 21-28.

Csanady, G. T. (1967b). "Variance of Local Concentration Fluctuations." *Boundary Layers and Turbulence, Physics of Fluids Supplement*, 576-578.

Csanady, G. T. (1973). *Turbulent Diffusion in the Environment*, D. Reidel Publ. Co., Boston.

Demetracopoulos, A. C., and Stefan, H. G. (1983). "Transverse Mixing in Wide and Shallow River: Case Study." *J. Hydr. Div.*, ASCE, 109(3), 685-699.

Dimou, K. N., and Adams, E. E. (1994). "A Random-Walk, Particle Tracking Model for Well-mixed Estuaries and Coastal Waters." *Est., Coastal and Shelf Sc.*, 37, 99-110.

Elder, J. W. (1959). "The Dispersion of Marked Fluid in Turbulent Shear Flow." *J. Fluid Mech.*, 5, 544.

Elkinton, J. S., Carde, R. T., Mason, C. J. (1984). "Evaluation of Time-average Dispersion Models for Estimating Pheromone Concentration in a Deciduous Forest." *J. Chem. Ecol.*, 10, 1081-1108.

Fackrell, J. E., and Robins, A. G. (1982). "Concentration Fluctuations and Fluxes in Plumes from Point Sources in a Turbulent Boundary Layer." *J. Fluid Mech.*, 117, 1-26.

Feynman, R. P., Leighton, R. B., and Sands, M. (1963). *The Feynman Lectures on Physics*, Addison Wesley, New York.

Fischer, H. B., List, E. J., Koh, R. C. Y., Imberger, J., and Brooks, N. H. (1979). *Mixing in Inland and Coastal Waters*, Academic Press, New York.

Gifford, F. A. (1959). "Statistical Properties of a Fluctuating Dispersion Model." in *Atmospheric Dispersion and Air Pollution*, F. N. Frankiel and P. A. Sheppard, Editors, Academic Press, 117.

Hanna, S. R. and Insley, E. M. (1989). "Time Series Analysis of Concentration and Wind Fluctuations." *Boundary-Layer Meteorology*, 47, 131-147.

Gifford, F. A. (1960). "Peak to average concentration ratios according to a fluctuating plume dispersion model." *Int. J. Air Poll.*, 3, 253.

Holley, E. R., and Jirka, G. H. (1986). "Mixing in Rivers." Tech Rept. No. E-86-11, U.S. Army Corps of Engineers, Vicksburg, Miss.

Holly, F. M., and Nerat, G. (1983). "Field Calibration of Stream-Tube Dispersion Model." *J. Hydr. Div.*, ASCE, 109, 1455.

Jeng, S. W., and Holley, E. R. (1986). "Two-Dimensional Random Walk Model for Pollutant Transport in Natural Rivers." Center for Research in Water Resources, Univ. of Texas, Austin, Texas.

Jobson, H. E., and Sayre, W. W. (1970). "Vertical Transfer in Open Channel Flow." *J. Hydr. Div.*, ASCE, 96, 703.

Jones, C. D. (1983). "On the Structure of Instantaneous Plumes in the Atmosphere." *J. Hazardous Materials*, 7, 87-112.

Luhar, A. K., and Sawford, B. L. (1995). "Lagrangian Stochastic Modeling of the Coastal Fumigation Phenomenon." *J. Appl. Meteor.*, 34, 2259-2277.

Luhar, A. K., and Britter, R. E. (1992). "Random-walk Modeling of Buoyant-plume Dispersion in the Convective Boundary Layer." *Atmospheric Environment*, 26A(7), 1283-1298.

Moore, P. A. and Atema, J. (1991). "Spatial Information in the Three-Dimensional Fine Structure of an Aquatic Odor Plume." *Biol. Bull.*, 181, 408-418.

Murlis, J. (1986). "The Structure of Odour Plumes." in *Mechanisms in Insect Olfaction*, T. L. Payne, M. C. Birch, and C. E. J. Kennedy, Editors, Oxford: Clarendon.

Murlis, J., and Jones, C. D. (1981). "Fine-scale Structure of Odour Plumes in Relation to Insect Orientation to Distant Pheromone and Other Attractant Sources." *Physiological Entomology*, 6, 71-86.

Mylne, K. R., Davidson, M. J., and Thomson, D. J. (1996). "Concentration Fluctuation Measurements in Tracer Plumes using High and Low Frequency Response Detectors." *Boundary-Layer Meteorology*, 79, 225-242.

Nakamura, I., Sakai, Y., and Miyata, M. (1987). "Diffusion of Matter by a Non-buoyant Plume in Grid-generated Turbulence." *J. Fluid Mech.*, 178, 379-403.

Nokes, R. I., and Wood, I. R. (1988). "Vertical and Lateral Turbulent Dispersion; Some Experimental Results." *J. Fluid Mech.*, 187, 373-394.

Pasquill, F., and Smith, F. B. (1983). "Atmospheric diffusion," E. Horwood, New York.

Pearce, B. R., et al. (1990). "Thermal Plume Study in the Delaware River: Prototype Measurements and Numerical Simulation." *IAHR International Conference on Physical Modeling of Transport and Dispersion*, 13B.7-13B.12, Cambridge, Mass.

Pernik, M. (1985). *Mixing Processes in a River-Floodplain System*, M. S. Thesis, School of Civil Engineering, Georgia Institute of Technology, Atlanta.

Petrenko, A. A., Jones, B. H., and Dickey, T. D. (1998). "Shape and Initial Dilution of the Sand Island, Hawaii Sewage Plume." *J. Hydr. Eng.*, ASCE, 124(6), 565-571.

Rahman, S., Dasi, L. P., Webster, D. R., and Roberts, P. J. W. (2000). "Characteristics of Turbulent Plumes using PLIF Technique." *2000 ASCE Joint Conference on Water Resources Engineering and Water Resources Planning & Management*, Minneapolis, MN.

Reeder, P. B., and Ache, B. W. (1980). "Chemotaxis in the Florida Spiny Lobster, *Panulirus argus*." *Anim. Behav.*, 28, 831-839.

Richardson, L. F. (1926). "Atmospheric Diffusion Shown on a Distance-neighbor Graph." *Proc. Roy. Soc. London*, A110, 709-739.

Roberts, P. J. W. (1996). "Sea Outfalls." in *Environmental Hydraulics*, V. P. Singh and W. Hager, Editors, Kluwer Academic Publishers, Dordrecht.

Roldao, J., Carvalho, J. L. B., and Roberts, P. J. W. (2000). "Field Observations of Dilution on the Ipanema Beach Outfall." *1st World Congress of the IWA*, Paris.

Smith, R. (1981). "Effect of Non-Uniform Currents and Depth Variations upon Steady Discharges in Shallow Water." *J. Fluid Mech.*, 110, 373.

Taylor, G. I. (1921). "Diffusion by Continuous Movements." *Proc. London Math. Soc.*, 2(20), 196.

Webel, G., and Schatzmann, M. (1984). "Transverse Mixing in Open Channel Flow." *J. Hydr. Eng.*, ASCE, 110(4), 423-435.

Webster, D. R., Rahman, S., and Dasi, L. P. (2001). "On the Usefulness of Bilateral Comparison to Tracking Turbulent Chemical Odor Plumes." To appear in *Limnology and Oceanography*.

Webster, D. R., Roberts, P. J. W, Rahman, S., and Dasi, L. P. (1999). "Simultaneous PIV/PLIF Measurements of a Turbulent Chemical Plume." *1999 International Water Resources Engineering Conference*, Seattle, WA.

Webster, D. R., Roberts, P. J. W., and Ra'ad, L. (2001). "Simultaneous DPTV/PLIF Measurements of a Turbulent Jet." *Experiments in Fluids*, 30(1), 65-72.

Weissburg, M. J. (2000). "The Fluid Dynamical Context of Chemosensory Behavior." *Biol. Bull.*, 198, 188-202.

Weissburg, M. J., and Zimmer-Faust, R. K. (1994). "Odor Plumes and How Blue Crabs Use Them in Finding Prey." *J. Experimental Biology*, 197, 349-375.

Yee, E., Wilson, D. J., and Zelt, B. W. (1993). "Probability Distributions of Concentration Fluctuations of a Weakly Diffusive Passive Plume in a Turbulent Boundary Layer." *Boundary-Layer Meteorology*, 64, 321-354.

Yotsukura, N., and Sayre, W. W. (1976). "Transverse Mixing in Natural Channels." *Water Resour. Res.*, 12(4), 695-704.